

## Influence of mechanochemical activation of metal-doped ZnO on its photocatalytic activity in degradation of Malachite Green dye

K. I. Milenova<sup>1\*</sup>, K. L. Zaharieva<sup>1</sup>, A. E. Eliyas<sup>1</sup>, I. A. Avramova<sup>2</sup>, I. D. Stambolova<sup>2</sup>, V. N. Blaskov<sup>2</sup>, O. S. Dimitrov<sup>3</sup>, S. V. Vassilev<sup>3</sup>, Z. P. Cherkezova-Zheleva<sup>1</sup>, S. K. Rakovsky<sup>1</sup>

<sup>1</sup> Institute of Catalysis, Bulgarian Academy of Sciences, Acad. G. Bonchev St., Bldg. 11, 1113 Sofia, Bulgaria

<sup>2</sup> Institute of General and Inorganic Chemistry, Bulgarian Academy of Sciences, Acad. G. Bonchev St., Bldg. 11, 1113 Sofia, Bulgaria

<sup>3</sup> Institute of Electrochemistry and Energy Systems, Bulgarian Academy of Sciences, Acad. G. Bonchev St., Bldg. 10, 1113 Sofia, Bulgaria

Received: September 28, 2015; Revised December 15, 2015

Mechanochemical activation (MCA) of ZnO samples doped with Ag, Ni, or Co was studied with regard to effect on their photocatalytic activities in degradation of Malachite Green dye. The samples were characterized by XRD and XPS methods. XRD spectra of ZnO photocatalysts showed presence of wurtzite ZnO phase. After MCA, the degree of crystallization was increased and crystallite sizes were smaller. Ratios of defect oxygen species to total oxygen were calculated for mechanochemically treated doped ZnO catalysts and compared with those of matching non-activated ZnO catalysts using X-ray photoelectron spectra.

The rate of Malachite Green oxidative discoloration reaction on cobalt- and silver-doped ZnO increases with duration of post-synthesis mechanochemical treatment. Mechanochemical activation effect is strongest for silver-doped samples due to the smallest size of the crystallites and increased degree of crystallization.

**Keywords:** doping, mechanochemical activation, ZnO, photocatalysts, ultraviolet light.

### INTRODUCTION

Applying mechanochemical treatment procedures for tuning of the activity and physicochemical properties of materials has a significant evolution in recent years. Mechanochemical activation could be an effective route for improvement of the structural and catalytic properties of metal oxide nanoparticles and nanocomposites. Mechanically introduced energy can also create crystal defects such as Schottky or Frenkel defects or crystallographic shear planes which can lead to enhanced catalytic or photocatalytic activities [1]. This technique can improve the surface areas and porous structures. In many cases, mechanochemical nanomaterials and nanocatalysts exhibit comparable or improved catalytic activities as compared to conventionally synthesized materials.

Air and water pollution with persistent organic pollutants can cause significant health and environmental problems. In many cases, conventional purification techniques are not effective. Photocatalysis using inorganic semiconductors is considered to have significant potential to destroy organic pollutants in wastewaters [2]. Recently, ZnO photocatalyst is attracting increased attention due to its

similarity with TiO<sub>2</sub> in band gap, high quantum efficiency, and high photocatalytic activity [3]. Doping is a widely applied procedure to diminish the wide band gap of ZnO and reduce the electron-hole recombination rate of ZnO during the photocatalytic process by using various transition or noble metals such as Cu, Ni, Co, Mn, Ag, *etc.* [4]. Saharan *et al.* [5] have obtained nickel-doped ZnO by chemical precipitation method applying CTAB surfactant at a low temperature. They found that substitutional doping of Ni in ZnO lattice at low temperatures has a positive influence on ZnO electronic structure and improved photocatalytic activity for degradation of anionic (Fast Green) and cationic (Victoria Blue) dyes.

Nickel-ZnO hybrid nanostructures, prepared by reduction of nickel chloride hexahydrate through a solvothermal process followed by surface modification, act as an efficient photocatalyst for decomposition of Methylene Blue (MB) dye [6].

Nanorods of cobalt-doped ZnO, synthesized by hydrothermal method, exhibit a high photocatalytic activity in degradation of methylene blue dye and phenol [4].

Silver-doped ZnO nanorods were synthesized through the precipitation method and their photocatalytic activities at different doping levels were evaluated in the degradation of methylene blue [7].

\* To whom all correspondence should be sent  
E-mail: kmilenova@ic.bas.bg

It has been found that Ag doping leads to optical band gap narrowing. Silver-deposited ZnO nanoparticles (NPs) have been synthesized by sol-gel method designed for visible light excited photocatalytic degradation of methylene blue [8]. Ag/ZnO NPs exhibit a five-fold higher activity than the pristine ZnO and four times greater than that of reference Degussa P-25. A high visible-light activity of Ag/ZnO could be attributed to effective charge separation. Dimitriev *et al.* [9] have performed soft mechanochemical synthesis of ZnO powders to avoid formation of intermediate ZnCO<sub>3</sub> and additional heat treatment. The mechanochemically synthesized ZnO powders possess good photocatalytic properties for degradation of Malachite Green dye.

The purpose of the present study was to perform mechanochemical activation (MCA) of doped ZnO powders and test their photocatalytic activities toward degradation of Malachite Green dye.

## EXPERIMENTAL

Activated ZnO powder samples, doped with 1.5 wt.% Co, Ni or Ag, were prepared using zinc carbonate precursor [10]. The procedure comprised thermal decomposition at 400°C followed by impregnation with the corresponding metal nitrate. Doped samples were finally calcined in air at 500°C for 2 h. The so obtained Co-, Ni- and Ag-doped ZnO samples were mechanochemically treated in a high-energy planetary ball mill (model PM 100, Retsch, Germany). The mechanochemical activation was carried out in an agate-milling container of 80-ml volume for milling time interval of 15 minutes at a milling speed of 400 rpm using air medium. The mass ratio of sample amount to applied balls was 1:9.

Sample morphology was examined on a JEOL model JEM-200CX scanning electron microscope equipped with an EM-ASID3D scanning adaptor.

An X-ray diffraction (XRD) investigation of the samples was performed using a Philips PW 1050 instrument with CuK $\alpha$  radiation. Crystallite sizes were determined by Scherrer formula.

X-ray photoelectron spectroscopy (XPS) studies were carried out in a VG Escalab II electron spectrometer using AlK $\alpha$  radiation with energy of 1486.6 eV under base pressure of 10<sup>-7</sup> Pa and a total instrumental resolution of 1 eV. Binding energies (BE) were determined using the C1s line (from adventitious carbon) as a reference with energy of 285.0 eV. The accuracy of measuring the BE values was 0.2 eV. C1s, Zn2p, and O1s photoelectron lines were recorded and corrected by subtracting Shirley's type of background and quantified using the peak area and Scofield's photoionization cross-sections.

The photocatalytic activities of the prepared samples were measured in the oxidative degradation of Malachite Green dye under UV light irradiation (power of 18 W, maximum emission at 365 nm) in a semi-batch photocatalytic reactor. Feeding large stoichiometric excess of oxygen allows modelling the kinetics of bimolecular reaction reducing it to a pseudo-first order rate equation, disregarding the dissolved oxygen concentration. Being practically constant, C<sub>O<sub>2</sub></sub> is included in the value of the apparent rate constant. The course of the photocatalytic reaction was followed using a UV-Vis absorbance spectrophotometer in the wavelength range from 200 to 800 nm. The initial concentration of the used MG dye solution was 5 ppm ( $\lambda_{\text{max}} = 615$  nm) and the catalyst loading was 1 g.L<sup>-1</sup>. Before UV illumination, the investigated systems were equilibrated in the dark for about 30 min. The rate constants *k* were evaluated as a slope of linear logarithmic dependence  $-\ln(C/C_0) = k_{\text{app}}t$ .

## RESULTS AND DISCUSSION

X-ray diffraction spectra have proved that all doped ZnO samples without mechanochemical treatment represent a wurtzite crystallographic phase (PDF 36-1451) with three main peaks corresponding to (100), (002), and (101) planes orientation [10]. Figure 1 displays XRD patterns of the samples after mechanochemical activation. The Ag/ZnO-MCA sample shows traces of silver oxide phase. The intensity of the crystallographic peaks of MCA samples is twice higher than that of the initial samples.

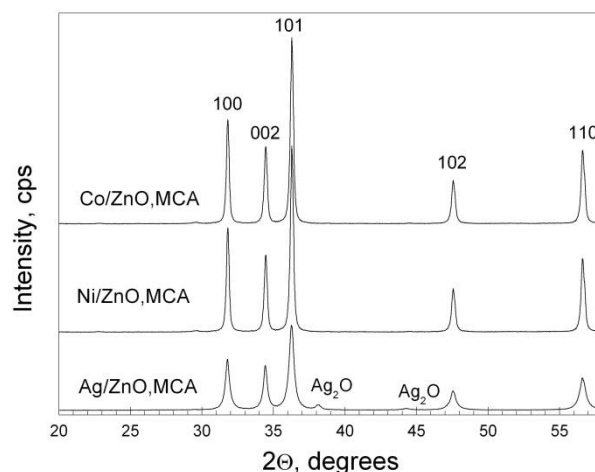


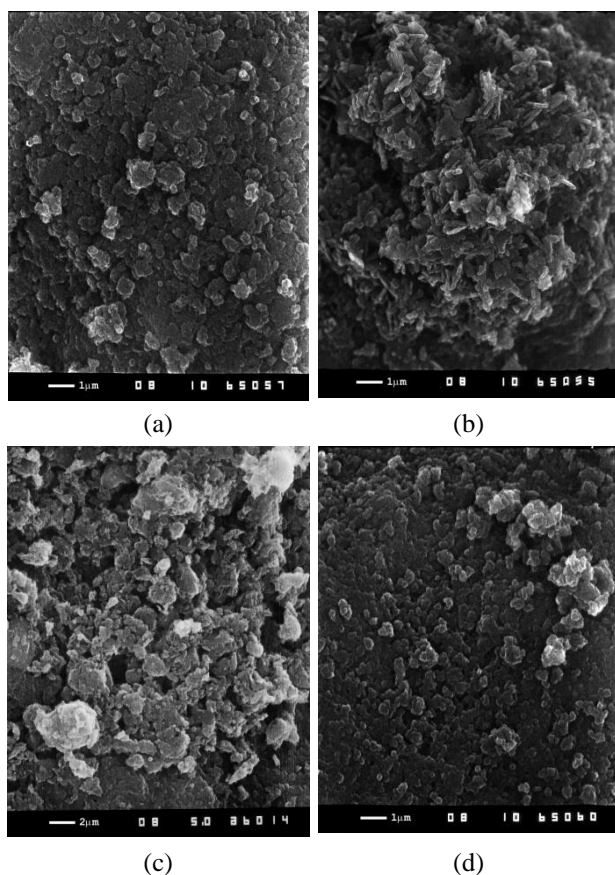
**Fig. 1.** X-ray diffraction patterns of mechanochemically activated samples

Mean crystallite sizes of fresh and mechanochemically activated samples are shown in table 1. The MCA leads to a strong decrease in crystallite sizes.

**Table 1.** Mean crystallites sizes (nm).

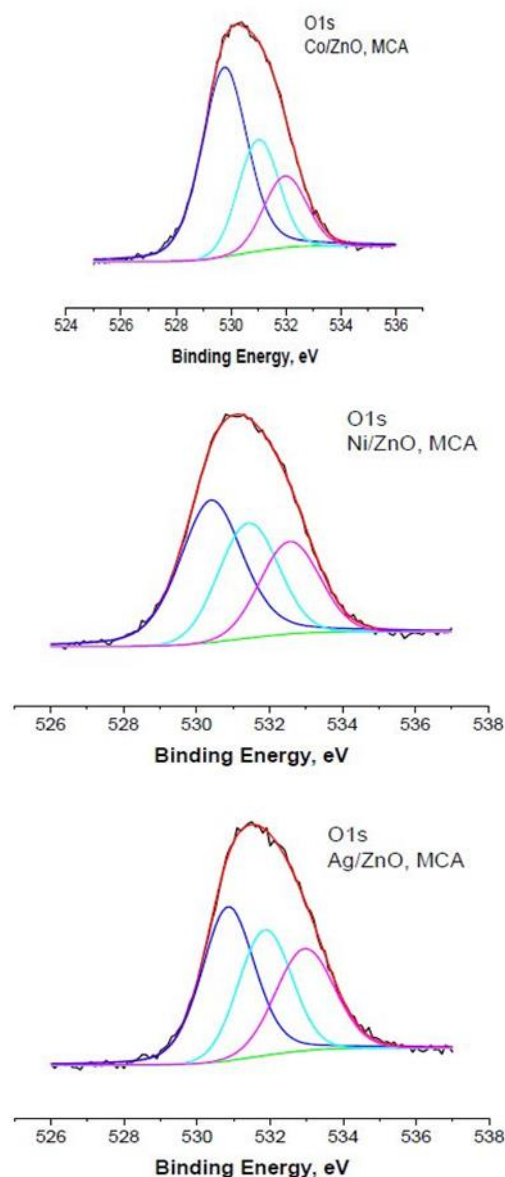
| Sample  | Before MCA | After MCA |
|---------|------------|-----------|
| Ni/ZnO  | 54         | 24        |
| Co/ ZnO | 52         | 24        |
| Ag/ZnO  | 50         | 22        |

Figure 2 shows SEM pictures of Ni/ZnO, Ni/ZnO-MCA, Ag/ZnO, and Ag/ZnO-MCA samples. Figures 2a,b represent surface morphology species of the Ni/ZnO and Ni/ZnO-MCA samples. It is seen that after mechanochemical activation the spheroidal species is transformed into needle-like crystals. In the case of Ag/ZnO (Figs. 2c,d) the effect of MCA is more strongly expressed. Particles size is being considerably reduced revealing internal surface and the rate of dye molecule diffusion is being increased, whereupon the inner pores become easily accessible. This brings about a higher rate of the photocatalytic reaction. The smaller particle size also causes a reduced degree of scattering of the light beam because of which the reaction is accelerated due to a greater number of active sites.

**Fig. 2.** SEM pictures of: (a) Ni/ZnO, (b) Ni/ZnO, MCA, (c) Ag/ZnO and (d) Ag/ZnO, MCA.

Surface chemical states of the elements in the mechanochemically activated ZnO photocatalysts doped with Ag, Co, and Ni were investigated by using an X-ray photoelectron spectroscopy method.

The most intensive photoelectron lines of zinc, oxygen as well as those of silver, cobalt, and nickel were studied. Recorded Ag3d, Co2p, and Ni2p photoelectron spectra (not shown here) were used to estimate dopant oxidation states as follows: Ag<sup>+</sup>, Co<sup>2+</sup>, and Ni<sup>2+</sup> [10]. O1s photoelectron lines obtained for the ZnO powders were complex and to understand their nature they were subjected additionally to a fitting procedure. The fitted O1s spectra presented in figure 3 manifest three peaks.

**Fig. 3.** XPS spectra of O1s for mechanochemically activated samples.

The peak at around 530.5 eV belongs to oxygen in stoichiometric ZnO, the second one at around 531.5 eV is attributed to oxygen in a non-stoichiometric ZnO matrix and the third peak (around 532.5 eV) is ascribed to chemisorbed oxygen: an OH group or dissociated oxygen on the surface of the

mechanochemically treated doped ZnO catalysts. Ratios of defect oxygen species to total oxygen were calculated for mechanochemically treated doped ZnO catalysts and compared with those of matching non-activated ZnO catalysts. Oxygen species associated with defects related to the total oxygen is increasing in the order: Ag/ZnO-MCA (30.5%) > Ni/ZnO-MCA (30.26%) > Co/ZnO-MCA (26%) > Ag/ZnO (25.3%) > Co/ZnO (23.9%) > Ni/ZnO (20.8%). It is worth mentioning that the mechanochemical activation procedure obviously leads to creation of more oxygen vacancies on the surface of silver-, cobalt-, and nickel-doped ZnO catalysts.

A previous study of mechanochemically activated ZnO powders doped with nickel, cobalt, and silver reports a positive effect on photocatalytic performance for degradation of azo dye RB5 over doped samples, as compared with undoped ZnO in all cases [10]. Degradation rate constants were calculated and increased in the following order: ZnO < Co-ZnO < Ag-ZnO < Ni-ZnO. This confirms the most positive effect of nickel dopant on the photocatalytic properties of activated ZnO. Figures 4 and 5 illustrate the reaction course of Malachite Green dye solution under UV-A illumination over Ni/ZnO, Co/ZnO, Ag/ZnO, Ni/ZnO-MCA, Co/ZnO-MCA, and Ag/ZnO-MCA catalysts. Malachite Green dye was used as a model pollutant due to its carcinogenic and teratogenic effect [11, 12].

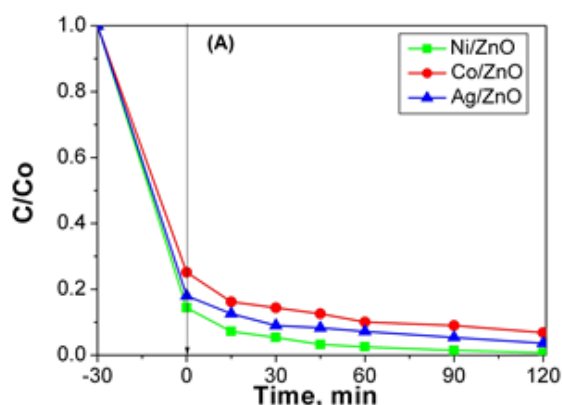


**Fig. 4.** Reaction course of the Malachite Green dye solution under UV-A illumination of (A) Ni/ZnO; Co/ZnO; Ag/ZnO.

The photocatalytic activities of the samples depended both on dopant type and applied activation treatment. Among all the investigated dopants, the nickel doping of ZnO powders affected most favourably the rate of oxidative discoloration reaction of the Malachite Green dye solution. It can be supposed that nickel doping in a semiconductor shifts the Fermi level towards more negative potential and improves the efficiency of the interfacial charge transfer process [13]. Therefore, the transfer

of an electron that takes place from the conduction band of ZnO to the new Fermi level is facilitated in the Ni-doped ZnO, as shown in Ref. 6. Such an electron transfer between the photoexcited semi-conducting ZnO and the dopant prevents electron-hole recombination [14]. As a result, enhanced photodegradation of the dye is observed.

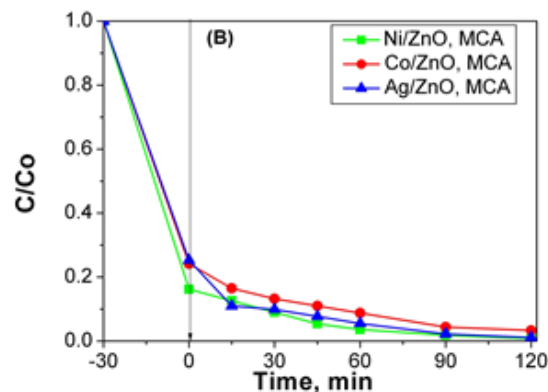


**Fig. 5.** Reaction course of the Malachite Green dye solution under UV-A illumination of (B) Ni/ZnO, MCA; Co/ZnO, MCA; Ag/ZnO, MCA.

Mechanochemically treated Ag- or Co-doped powders increase the photocatalytic efficiency of the samples. This effect was more pronounced in the case of Ag/ZnO-MCA powders. After 120 min of illumination, the conversion degree of dye degradation was 99%, while for the non-treated samples it was 96%. The higher efficiency of mechanically activated Ag/ZnO samples is attributed to enhanced crystallization and a decrease in crystallite size [15].

Figure 6 compares rate constants of the photocatalytic process in presence of the investigated catalysts under UV-A illumination. The photocatalytic activity of ZnO nanomaterials is strongly dependent on porous structure, presence of defects, crystallite size, degree of crystallinity, etc., which are affected by the preparation procedure [15]. The best photocatalytic properties of Ag/ZnO-MCA samples can be ascribed to smaller crystallite sizes and enhanced crystallization in comparison with non-activated Ag/ZnO.

SEM pictures displayed in figure 2d reveal that the Ag/ZnO-MCA sample exposes sphere-like particles that enhanced photocatalytic performance [16, 17] without being aggregates as Ag/ZnO. Aggregation leads to suppression of photocatalytic activity because it can lead to fewer electron-hole pairs, which result in suppressed OH• generation, as in the case of Ni/ZnO-MCA [18]. Another possible reason is associated with aggregate particle size distribution, which may influence both light absorption and light scattering mechanisms that determine the degree of photon interaction with photocatalyst

particles. Scattered light intensity is probably stronger on samples with aggregates.

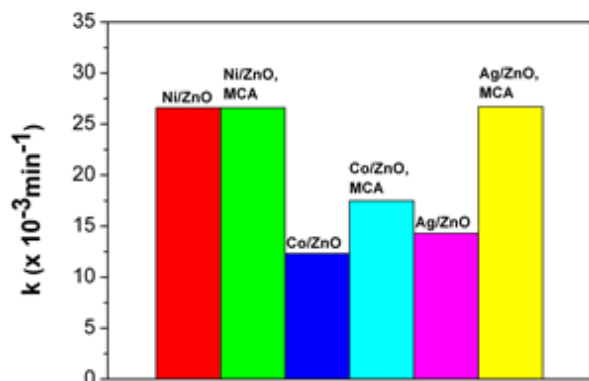


**Fig. 6.** Rate constants  $k$  of the photocatalytic process in the presence of the investigated catalysts under UV-A illumination.

## CONCLUSIONS

Mechanochemical post-synthesis activation of metal-doped (Ag, Co or Ni) ZnO powders was investigated in connection with their photocatalytic activities in degradation of Malachite Green dye. An increased degree of crystallization and decreased crystallite sizes of the samples were observed after mechanochemical activation. The mechanochemical treatment results in formation of a larger number of oxygen defects in the ZnO lattice, which play the role of adsorption sites. Degradation apparent rate constants (pseudo-first order kinetics) are decreasing in the following order: Ag/ZnO-MCA ( $26.7 \times 10^{-3} \text{ min}^{-1}$ ) > Co/ZnO-MCA ( $17.5 \times 10^{-3} \text{ min}^{-1}$ ) > Ag/ZnO ( $14.3 \times 10^{-3} \text{ min}^{-1}$ ) > Co/ZnO ( $12.3 \times 10^{-3} \text{ min}^{-1}$ ). The mechanochemical activation promotes significantly the rate of oxidative reaction of Malachite Green dye discoloration in the case of samples doped with silver.

*Acknowledgements:* The authors gratefully acknowledge financial support by the Bulgarian Science Fund (Contracts DFNI-T-02-16 and DFNI-E-02-2/2014) and the collateral contract between

Bulgarian Academy of Sciences and Serbian Academy of Sciences and Arts 'Development of advanced catalytic systems applicable to chemical and photochemical processes for neutralization of environmental pollution'

## REFERENCES

1. C. Xu, S. De, A. M. Balu, M. Ojeda, R. Luque, *Chem. Commun.*, **51**, 6698 (2015).
2. R. Chauhan, A. Kumar, R. P. Chaudhary, *J. Sol-Gel Sci. Technol.*, **63**, 546 (2012).
3. L. Saiki, D. Bhuyan, M. Saikia, B. Malakara, D. K. Dutta, P. Sengupta, *Appl. Catal. A-Gen.*, **490**, 42 (2015).
4. B. M. Rajbongshia, S. K. Samdarshi, *Mater. Sci. Eng. B*, **182**, 21 (2014).
5. P. Saharan, G. R. Chaudhary, S. Lata, S.K. Mehta, S. Mor, *Ultrason. Sonochem.*, **22**, 317 (2015).
6. S. Senapati, S. K. Srivastava, S. B. Singh, *Nanoscale*, **4**, 6604 (2012).
7. R. Rahimi, J. Shokrayian, M. Rabbani, doi: 10.3390/ecsoc-17-b019.
8. B. Rajbongshi, A. Ramchiary, B. Jha, S. Samdarshi, *J. Mater. Sci.-Mater. Electron.*, **25**, 2969 (2014).
9. Y. Dimitriev, M. Gancheva, R. Iordanova, *J. Alloys Compd.*, **519**, 161 (2012).
10. K. Milenova, I. Avramova, A. Eliyas, V. Blaskov, I. Stambolova, N. Kassabova, *Environ. Sci. Pollut. Res.*, **21**, 12249 (2014).
11. R. Gopinathan, J. Kanhere, J. Banerjee, *Chemosphere*, **120**, 637 (2015).
12. S. Srivastava, R. Sinhaa, D. Roya, *Aquat. Toxicol.*, **66**, 319 (2004).
13. V. Subramanian, E. E. Wolf, P. V. Kamat, *J. Am. Chem. Soc.*, **126**, 4943 (2004).
14. R. Georgekutty, M. K. Seery, S. C. Pillai, *J. Phys. Chem. C*, **112**, 13563 (2008).
15. M. Fallet, S. Permpoon, J. L. Deschanvres, M. Langlet, *J. Mater. Sci.*, **41**, 2915 (2006).
16. A. Lei, B. Qu, W. Zhou, Y. Wang, Q. Zhang, B. Zou, *Mater. Lett.*, **66**, 72 (2012).
17. H. Liu, J. Yang, J. Liang, Y. Huang, C. Tang, *J. Am. Ceram. Soc.*, **91**, 1287 (2008).
18. D. Jassby, J. F. Budarz, M. Wiesner, *Environ. Sci. Technol.*, **46**, 6934 (2012).

## ВЛИЯНИЕ НА МЕХАНОХИМИЧНАТА АКТИВАЦИЯ НА ZnO ДОТИРАН С МЕТАЛ ВЪРХУ ФОТОКАТАЛИТИЧНАТА АКТИВНОСТ ЗА РАЗЛАГАНЕ НА БАГРИЛОТО МАЛАХИТОВО ЗЕЛЕНО

К. И. Миленова<sup>1\*</sup>, К. Л. Захариева<sup>1</sup>, Ал. Ел. Елияс<sup>1</sup>, Ив. А. Аврамова<sup>2</sup>, Ир. Д. Стамболова<sup>2</sup>,  
Вл. Н. Блъсков<sup>2</sup>, Ог. С. Димитров<sup>3</sup>, С. В. Василев<sup>3</sup>, З. П. Черкезова-Желева<sup>1</sup>, Сл. К. Раковски<sup>1</sup>

<sup>1</sup> *Институт по катализ, Българска академия на науките, ул. „Акад. Г. Бончев“, бл. 11, 1113 София, България*

<sup>2</sup> *Институт по обща и неорганична химия, Българска академия на науките, ул. „Акад. Г. Бончев“, бл. 11, 1113 София, България*

<sup>3</sup> *Институт по електрохимия и енергийни системи, Българска академия на науките, ул. „Акад. Г. Бончев“, бл. 10, 1113 София, България*

Постъпила на 28 септември 2015 г.; Преработена на 15 декември 2015 г.

(Резюме)

Изследван е ефектът на механохимичната активация на ZnO дотиран с Ag, Ni или Co върху фотокаталитичната му активност за разлагане на багрилото Малахитово Зелено. Образците са охарактеризирани чрез методите на рентгенова дифракция и рентгенова фотоелектронна спектроскопия. Рентгеновите спектри на фотокатализаторите от ZnO показаха присъствие на вюрцитна фаза. Степента на кристализация нараства, а размерите на кристалитите намаляват силно след механохимична активация. Изчислено е съотношението между кислорода принадлежащ на дефекти и общия кислород за механохимично активираните катализатори от дотиран ZnO и е сравнено със същата величина за нетретираните образци на основата на рентгеновите фотоелектронни спектри.

Скоростта на окислителната реакция водеща до обезцветяване на Малахитово зелено в присъствие на ZnO дотиран с кобалт или сребро нараства след механохимичната им обработка. Ефектът от механохимичната активация е най-силен за дотираните със сребро образци, което се дължи на малкия размер на кристалитите и по-високата степен на кристалност.